

Study of the  $\rho'$  (1600) Mass Region Using  $\gamma p \rightarrow \pi^+ \pi^- p$  at 20 GeV\*

## The SLAC Hybrid Facility Photon Collaboration

K.Abe<sup>m</sup>, T.C. Bacon<sup>e</sup>, J. Ballam<sup>k</sup>, A.V. Bevan<sup>e</sup>, H.H. Bingham<sup>o</sup>, J.E. Brau<sup>q</sup>,  
 K. Braune<sup>k</sup>, D. Brick<sup>b</sup>, W.M. Bugg<sup>g</sup>, J.M. Butler<sup>k</sup>, W. Cameron<sup>e</sup>, H.O. Cohn<sup>i</sup>,  
 D.C. Colley<sup>a</sup>, S. Dado<sup>l</sup>, R. Diamond<sup>d</sup>, P. Dingus<sup>o</sup>, R. Erickson<sup>k</sup>, R.C. Field<sup>k</sup>,  
 B. Franek<sup>j</sup>, N. Fujiwara<sup>h</sup>, R. Gearhart<sup>k</sup>, T. Glanzman<sup>k</sup>, J. J. Goldberg<sup>l</sup>, A.T.  
 Goshaw<sup>c</sup>, G. Hall<sup>e</sup>, E.R. Hancock<sup>j</sup>, T. Handler<sup>q</sup>, H.J. Hargis<sup>q</sup>, E.L. Hart<sup>q</sup>,  
 K. Hasegawa<sup>m</sup>, R. I. Hulsizer<sup>g</sup>, M. Jobes<sup>a</sup>, T. Kafka<sup>n</sup>, G.E. Kalmus<sup>j</sup>, D.P.  
 Kelsey<sup>j</sup>, T. Kitagaki<sup>m</sup>, W. Kowald<sup>c</sup>, A. Levy<sup>p</sup>, P. W. Lucas<sup>c</sup>, W.A. Mann<sup>n</sup>, E.  
 McCrory<sup>c</sup>, R. Merenyi<sup>n</sup>, R. Milburn<sup>n</sup>, C. Milstene<sup>g</sup>, K.C. Moffeit<sup>k</sup>, J.J. Murray<sup>k</sup>,  
 A. Napier<sup>n</sup>, S. Noguchi<sup>h</sup>, F. Ochiai<sup>f</sup>, S. O'Neale<sup>a</sup>, A.P.T. Palounek<sup>c</sup>, I.A. Pless<sup>g</sup>,  
 P. Rankin<sup>k</sup>, W.J. Robertson<sup>c</sup>, H. Sagawa<sup>m</sup>, T. Sato<sup>f</sup>, J. Schneps<sup>n</sup>, S.J. Sewell<sup>j</sup>,  
 J. Shank<sup>o</sup>, A.M. Shapiro<sup>b</sup>, R. Sugahara<sup>f</sup>, A. Suzuki<sup>f</sup>, K. Takahashi<sup>f</sup>, K. Tamai<sup>m</sup>,  
 S. Tanaka<sup>m</sup>, S. Tether<sup>g</sup>, W.D. Walker<sup>c</sup>, M. Widgoff<sup>b</sup>, C.G. Wilkins<sup>a</sup>, S. Wolbers<sup>o</sup>,  
 C.A. Woods<sup>e</sup>, A. Yamaguchi<sup>m</sup>, R.K. Yamamoto<sup>g</sup>, S. Yamashita<sup>h</sup>, Y. Yoshimura<sup>f</sup>,  
 G.P. Yost<sup>o</sup>, H. Yuta<sup>m</sup>

Submitted to Physical Review Letters

- a. Birmingham University, Birmingham, B15 2TT, England
- b. Brown University, Providence, Rhode Island, 02912
- c. Duke University, Durham, North Carolina, 27706
- d. Florida State University, Tallahassee, Florida, 32306
- e. Imperial College, London, SW7 2BZ, England
- f. National Laboratory for High Energy Physics (KEK),  
Oho-machi, Tsukuba-gun, Ibaraki 305, Japan
- g. Massachusetts Institute of Technology, Cambridge, Massachusetts, 02139
- h. Nara Womens University, Kita-uoya, Nishi-Machi  
Nara 630, Japan
- i. Oak Ridge National Laboratory, Oak Ridge, Tennessee, 37830
- j. Rutherford Appleton Laboratory, Didcot,  
Oxon OX11 0QX, England
- k. Stanford Linear Accelerator Center, Stanford University,  
Stanford, California, 94305
- l. Technion-Israel Institute of Technology, Haifa 32000, Israel
- m. Tohoku University, Sendai 980, Japan
- n. Tufts University, Medford, Massachusetts, 02155
- o. University of California, Berkeley, California, 94720
- p. University of Tel Aviv, Tel Aviv, Israel
- q. University of Tennessee, Knoxville, Tennessee, 37916

---

\*Work supported in part by the Department of Energy, contract DE-AC03-76SF00515, the Japan-U.S Co-operative Research Project on High Energy Physics under the Japanese Ministry of Education, Science and Culture; the Science and Engineering Research Council (United Kingdom), the U.S. National Science Foundation and the U.S.-Israel Academy of Sciences Commission for Basic Research.

## ABSTRACT

We have observed the  $\pi^+\pi^-$  decay of the  $\rho'(1600)$  in the production reaction  $\gamma p \rightarrow \rho' p$  at 20 GeV. Using a calculation which takes into account the interference of the  $\rho'$  with the  $\rho(770)$  and a Drell background, we find good evidence that this resonance is a radial excitation of the  $\rho(770)$ . The background interference strongly distorts the angular distributions predicted by a purely s-channel helicity conserving production mechanism. We measure  $m_0 = (1.55 \pm .07) \text{ GeV}/c^2$  and  $\Gamma_0 = (0.28 \pm_{-.08}^{+.03}) \text{ GeV}/c^2$ .

The study of radially excited  $q\bar{q}$  states provides important information about the QCD force, especially its long-range confining character. In particular, the data available about vector mesons containing heavy quarks ( $c\bar{c}$  or  $b\bar{b}$ ) have led to the formulation of long-range, confining, linear potentials modified by short-range effects due to one gluon exchange.<sup>1</sup> Although good information is available about the spectra of these  $\Psi$  and  $\Upsilon$  states, the radial excitations of vector mesons composed of light quarks ( $u\bar{u}$ ,  $d\bar{d}$ , and  $s\bar{s}$ ) have proved difficult to measure because of broad decay widths and interfering backgrounds.

We present new information about a possible radial excitation of the  $\rho(770)$  produced in the reaction

$$\begin{array}{c} \gamma p \rightarrow p \rho' \\ \quad \quad \quad \downarrow \\ \quad \quad \quad \pi^+ \pi^- \end{array} \quad (1)$$

Unlike previous photoproduction studies<sup>2-6</sup> of the  $\pi^+\pi^-$  decay mode of the  $\rho'$ , this experiment has full decay acceptance, and the analysis uses an interference of vector mesons with a Drell background to study the amplitude variation of the  $J^P = 1^-\pi^+\pi^-$  system in the mass range up to  $2.0 \text{ GeV}/c^2$ .

The data used in this analysis were obtained from an experiment performed in the SLAC Hybrid Facility exposed to photons produced by backscattering laser light from a 30 GeV electron beam<sup>7</sup>. The photon beam had a linear polarization of 52%, and an average energy of 19.3 GeV with a spread of 1.7 GeV (FWHM). The photon flux was measured using an  $e^+e^-$  pair spectrometer and, independently, by a total absorption lead-scintillator counter. Produced charged or neutral particles (except those in a narrow forward region dominated by  $\gamma \rightarrow e^+e^-$  conversions) triggered the recording of hadronic interactions. A

kinematic fit with three constraints was used to select the  $\gamma p \rightarrow \pi^+ \pi^- p$  events. Backgrounds were studied and found to be negligible after rejecting that 1.4 % of the events which had a better fit to  $\gamma p \rightarrow \pi^+ \pi^- \pi^0 p$ ,  $K^+ K^- p$ , or  $p \bar{p} p$ . The data were corrected for experimental detection and selection losses as a function of the production and decay variables of the  $\pi^+ \pi^-$  system. An important feature of the experiment is that it has good acceptance for all decay angles of  $\pi^+ \pi^-$  pairs with masses between 0.4 and 2.5  $\text{GeV}/c^2$ .

The final data sample consists of 20908  $\gamma p \rightarrow \pi^+ \pi^- p$  interactions. This represents a cross section of  $(11.1 \pm 0.9) \mu\text{b}$ . A small, well-isolated signal of  $\Delta(1232)$  production was observed and removed by rejecting 133 events with  $m_{p\pi^\pm} < 1.4 \text{ GeV}/c^2$ . The  $\pi^+ \pi^-$  mass distribution of the remaining events, presented in Figure 1, shows that this channel is dominated by  $\rho(770)$  production. We will briefly discuss the production and decay characteristics of the  $\rho(770)$  and then show that a second resonance at a  $\pi^+ \pi^-$  mass of 1.55  $\text{GeV}/c^2$  is required to describe the data.

The cross section for the reaction  $\gamma p \rightarrow \rho p$  is known to vary slowly with center of mass energy and rapidly with the square of the four-momentum transferred ( $t' = t - t_{min}$ ) from the photon to the  $\rho$ . The variation with  $\pi^+ \pi^-$  mass of the slope parameter,  $b$ , from fits of the form  $Ae^{bt'}$  to the experimental distribution  $d\sigma/dt'$ , is shown in Figure 2. We will return to a discussion of the dependence of  $b$  on the  $\pi^+ \pi^-$  mass, but note here that the slope is  $(7.5 \pm 0.2) (\text{GeV}/c)^{-2}$  at the  $\rho$  mass peak. This value is typical of elastic processes, and suggests that the  $\rho$  is produced by the diffractive, vector meson dominance mechanism shown in Figure 3a.

The decay angular distributions<sup>8</sup> of the  $\rho$  in its helicity frame are shown

in figures 4a and 4b. As has been observed at lower energies, these angular distributions are consistent with  $\rho$  production via  $s$ -channel helicity conservation (SCHC) with natural spin-parity exchange.<sup>9,10,11</sup> The SCHC prediction for  $N_T$  events is given by  $d^2N/d\cos\Theta d\Psi = (3N_T/8\pi) \sin^2\Theta (1 + P_\gamma \cos 2\Psi)$ , where  $\Psi = \phi_E - \phi$ ,  $\Theta$  and  $\phi$  are the  $\rho$  helicity frame polar and azimuthal angles,  $\phi_E$  is the  $\rho$  azimuthal production angle with respect to the electric field vector of the photon, and  $P_\gamma$  is the degree of linear polarization of the incident photon. Fitting the data to this form yields  $P_\gamma = 0.49 \pm 0.02$  for  $t' < 0.4$  (GeV/c)<sup>2</sup> and  $0.7 < m_{\pi\pi} < 0.75$  GeV/c<sup>2</sup>. We expect  $P_\gamma = 0.52$  from the backscattered laser beam. Therefore, near the  $\rho$  peak, the  $\gamma p \rightarrow \rho p$  production process is essentially pure SCHC.

Away from the  $\rho$  peak, the data deviate from the prediction of pure diffractive  $\rho$  production. This may be due to the interference of the  $\rho$  amplitude with the Drell amplitude (shown in Figure 3b), as has been suggested by Söding<sup>12</sup> and verified in several  $\rho$  photoproduction experiments.<sup>10,11,13,14,15,16</sup> This interference is constructive below the  $\rho$  peak and destructive above, leading to the asymmetric  $\pi^+\pi^-$  mass distribution shown in Figure 1 and the rapidly varying  $t'$  slope shown in Figure 2.

We used the Söding model to examine these effects more quantitatively. The  $\rho$  production amplitude was taken to be purely imaginary and proportional to  $e^{bt'}/2$ . The  $\rho$  decay was described by a relativistic Breit-Wigner resonance with mass 0.769 GeV/c<sup>2</sup> and width 0.154 GeV/c<sup>2</sup>.<sup>17</sup> The Drell amplitude was calculated using  $\pi p \rightarrow \pi p$  phase shift data.<sup>18</sup> The relative intensity of the two  $\pi^+\pi^-$  production amplitudes and the  $t'$  slope  $b$  were treated as free parameters. The resulting predictions for the  $m_{\pi\pi}$  and  $t'$  distributions, normalized to the total

number of events, were fitted to the data. The results of this fit, with  $b = (7.0 \pm 0.4) (\text{GeV}/c)^{-2}$ , are given by the solid curves in Figures 1, 2, 4a and 4b. There is good agreement with the data except in the mass range between 1.3 and 1.8  $\text{GeV}/c^2$ , where there is a large  $\pi^+\pi^-$  mass enhancement above the predicted background and a rapid increase in the  $t'$  slope from about 1  $(\text{GeV}/c)^{-2}$  to about 5  $(\text{GeV}/c)^{-2}$ . These features strongly suggest the diffractive production of at least one additional resonance.

We next modify the model by adding a second  $J^P = 1^-$  resonance,  $\rho'$ , that is assumed to be produced in the same diffractive, SCHC manner as the  $\rho(770)$ . Within the context of the vector meson dominance model, this amplitude represents a sum of the two diagrams shown in Figures 3c and 3d. The free parameters in this extended Söding calculation are the intensity, mass, and width of the  $\rho'$ , and an overall sign of the  $\rho'$  production amplitude.

The results of this fit to the  $\pi^+\pi^-$  mass distribution are shown by the dashed curve in Figure 1. The data are best fit by a second resonance with  $m_0 = (1.55 \pm .07) \text{GeV}/c^2$  and  $\Gamma_0 = (0.28 \pm_{.08}^{.03}) \text{GeV}/c^2$ . The fit also requires that the sign of the  $\rho'$  production amplitude be negative relative to that of the  $\rho$ .<sup>19</sup> The model reproduces the observed bump in the  $t'$  slope, as shown by the dashed curve in Figure 2. The decay angular distributions in the  $\rho'$  mass region are shown in Figures 4c and 4d, as are the extended model predictions. The Drell background interference strongly distorts the pure SCHC prediction, and the model reproduces the decay angular distributions reasonably well. We can conclude from the  $\cos\Theta$  distribution shown in Figure 4c, that the  $\rho'$  is strongly aligned in the helicity frame. However, at the present statistical level, it is difficult to determine the extent of s-channel polarization from the  $\Psi$  distribution shown in Figure 4d. We

also note that earlier experiments with less than full angular acceptance would have had difficulty correcting for losses by simply assuming  $d\sigma/d\cos\Theta \propto \sin^2\Theta$  in the  $\rho'$  mass region.

We have also calculated the  $a_\ell^m(m_{\pi\pi})$  coefficients from a fit of our data to spherical harmonics. A comparison of these data with the extended Söding model shows good agreement for  $m_{\pi\pi}$  less than  $2.0 \text{ GeV}/c^2$ . In particular, no  $\pi^+\pi^-$  partial waves with  $\ell$  greater than one are required in addition to those introduced by the Drell amplitude.

In conclusion, we have observed a resonance with mass  $(1.55 \pm 0.07) \text{ GeV}/c^2$ , width  $(0.28 \pm_{.08}^{.03}) \text{ GeV}/c^2$ , and  $J^{PC} = 1^{--}$  in  $\gamma p \rightarrow \pi^+\pi^-p$ . The production characteristics of this state are similar to those of the  $\rho(770)$ . These facts suggest that this resonance is a radial excitation of the  $\rho(770)$ , although we can not rule out a  ${}^3D_1$ ,  $q\bar{q}$  meson. We find  $\sigma(\gamma p \rightarrow \rho' p) \times \text{BR}(\rho' \rightarrow \pi^+\pi^-)/\sigma(\gamma p \rightarrow \rho(770)p) = (1.34 \pm 0.23) \times 10^{-2}$  at  $E_\gamma = 19.3 \text{ GeV}$ . A future report will discuss our analysis of these data in more detail and include a measurement of the  $4\pi$  decay of this resonance.

We wish to thank the SLAC bubble chamber crew for their dedication and performance under difficult conditions, and the film scanners and measurers for their careful processing of the events. We have benefited from discussion of the theory of vector meson production with V. Barger, F.J. Gilman, M.-Y. Han, D.C. Peaslee, and J. Pumplin. This work was supported by the Japan-U.S. Cooperative Research Project on High Energy Physics under the Japanese Ministry of Education, Science, and Culture, the U.S. Department of Energy, the Science and Engineering Research Council (United Kingdom), the U.S. National Science Foundation and the U.S.-Israel Academy of Sciences Commission for Basic Research.



## FOOTNOTES

1. see, for example  
W. Buchmuller and S.-H.H.Tye, Phys. Rev. D24 (1981) 132, and  
E. Eichten et al., Phys. Rev. D21 (1980) 203, and  
S.N. Gupta et al., Phys. Rev. D26 (1982) 3305, and  
K. Berkelman, in High Energy Physics – 1980. Proceedings of the XXth  
International Conference, Madison, Wisconsin, edited by  
L. Durand and L.G. Pondrom (AIP, New York, 1981) p. 1500.
2. F. Bulos et al., PRL 26 (1971) 149.
3. H. Alvensleben et al., PRL 26 (1971) 273.
4. G. Alexander et al., Phys. Lett. 57B (1975) 487.
5. M.S. Atiya et al., PRL 43 (1979) 1691.
6. D. Aston et al., Phys. Lett. 92B (1980) 215.
7. K. Abe et al., SLAC-PUB 3271 (1983), submitted to Phys. Rev. D, J.E.  
Brau et al., NIM 196 (1982) 403.
8. The angular distributions shown come from a portion of the experiment  
where the photon polarization was uniformly about 50%. This consisted  
of 16331 events, 78% of the total.
9. Cambridge Bubble Chamber Group, Phys. Rev. 146 (1966) 994.
10. Y. Eisenberg et al., Phys. Rev. D5 (1972) 15.
11. J. Ballam et al., Phys. Rev. D7 (1973) 3150. See footnote 25 of this  
reference for a detailed description of the decay angles  $\Theta$  and  $\Psi$ .
12. P. Söding, Phys. Lett. 19 (1966) 702, see also A.S. Krass, Phys. Rev. 159  
(1967) 1496 and Jon Pumplin, Phys. Rev. D2 (1970) 1859.

13. H.H. Bingham, et al., PRL 24 (1970) 955, J. Ballam et al., PRL 24 (1970) 960, 1467 (E) (1970).
14. Aachen-Berlin-Bonn-Hamburg-Heidelberg-München Collaboration, Phys. Rev. 175 (1968) 1669.
15. G. McClellan et al., Phys. Rev. D4 (1971) 2683.
16. C. Berger et al., Phys. Lett. 39B (1972) 659.
17. J.D. Jackson, Nuovo Cimento 34 (1964) 1644. We used a mass dependent resonance width given by  $\Gamma = \Gamma_0 (q/q_0)^3 2q_0^2/(q^2 + q_0^2)$  where  $q$  is the  $\pi$  momentum in the  $\pi^+\pi^-$  center of mass system ( $q_0$  that at the resonant mass).
18. G. Höhler et al., Handbook of Pion-nucleon Scattering, University of Karlsruhe, No. 12/1 (1979).
19. If the  $\gamma p \rightarrow \rho p$  and  $\gamma p \rightarrow \rho' p$  production amplitudes were in phase, this measurement would imply that  $g_{\rho' p \pi} / g_{\rho p \pi}$  is negative. We note that this result may be related to the observation that the  $\rho$  and  $\rho'$  amplitudes must have opposite signs if VMD calculations of proton and pion electromagnetic form factors are to agree with measurements.

## FIGURE CAPTIONS

1. The  $\pi^+\pi^-$  invariant mass distribution corrected for all losses. The solid curve is the prediction of the Söding model with only the  $\rho(770)$  resonance. The dashed curve shows the effect of adding a second resonance of mass  $1.55 \text{ GeV}/c^2$  and width  $0.28 \text{ GeV}/c^2$ .
2. Variation of the four-momentum slope parameter,  $b$ , with  $\pi^+\pi^-$  mass. The curves are Söding model predictions with one (solid curve) and two (dashed curve) resonances as described in the text.
3. a) Diffractive production of the  $\rho(770)$ .  
b) Non-resonant  $\pi^+\pi^-$  production via a Drell amplitude as suggested by Söding.  
c) and d) Diffractive  $\rho'$  production amplitudes.
4. Decay angular distributions of the  $\pi^+\pi^-$  system in its helicity frame.  
a) and b) are for the  $\rho(770)$  mass region,  $.70 < m_{\pi\pi} < .80 \text{ GeV}/c^2$ .  
c) and d) are for the  $\rho'$  mass region,  $1.4 < m_{\pi\pi} < 1.8 \text{ GeV}/c^2$ .  
The  $p\pi^+$  mass cut ( $m_{p\pi^\pm} > 1.4 \text{ GeV}/c^2$ ) does not affect the  $\cos\Theta$  distribution in a) but removes events with  $|\cos\Theta| > 0.95$  in c). The curves are predictions of the Söding model as described in the text.

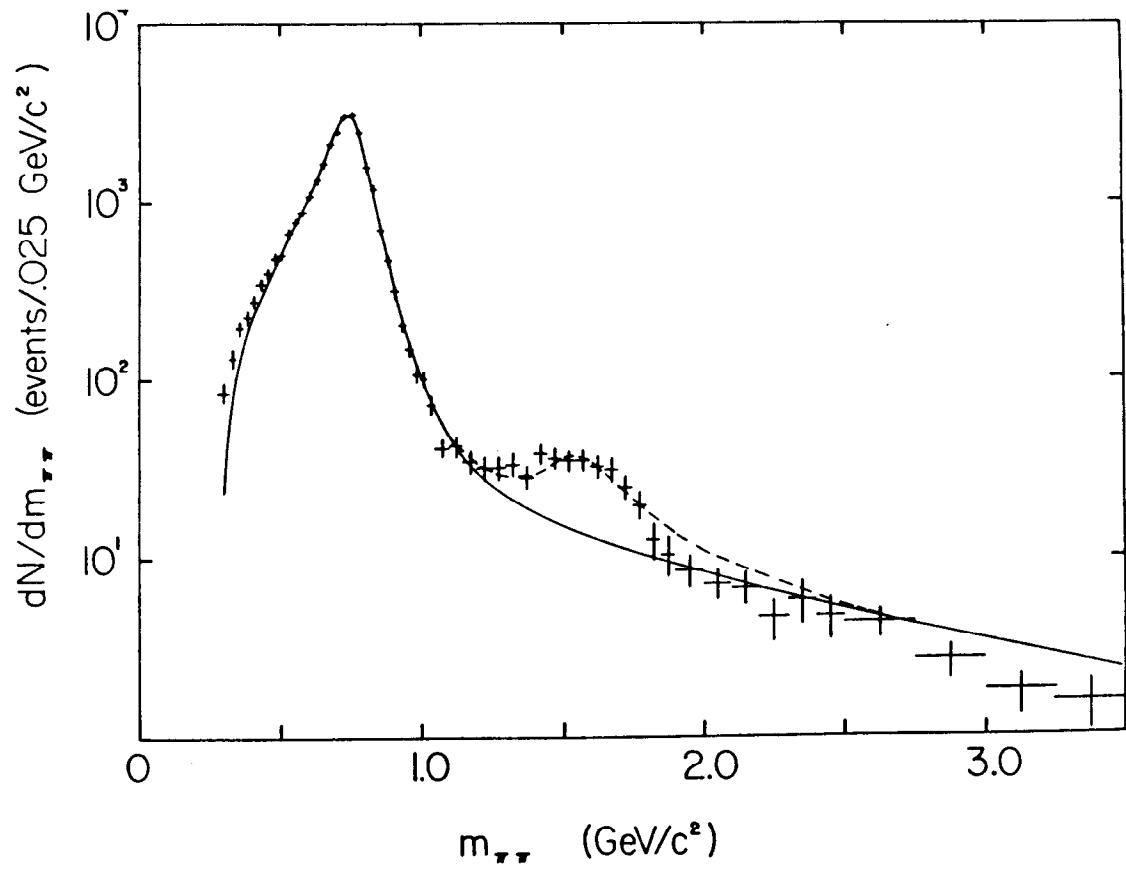


Fig. 1

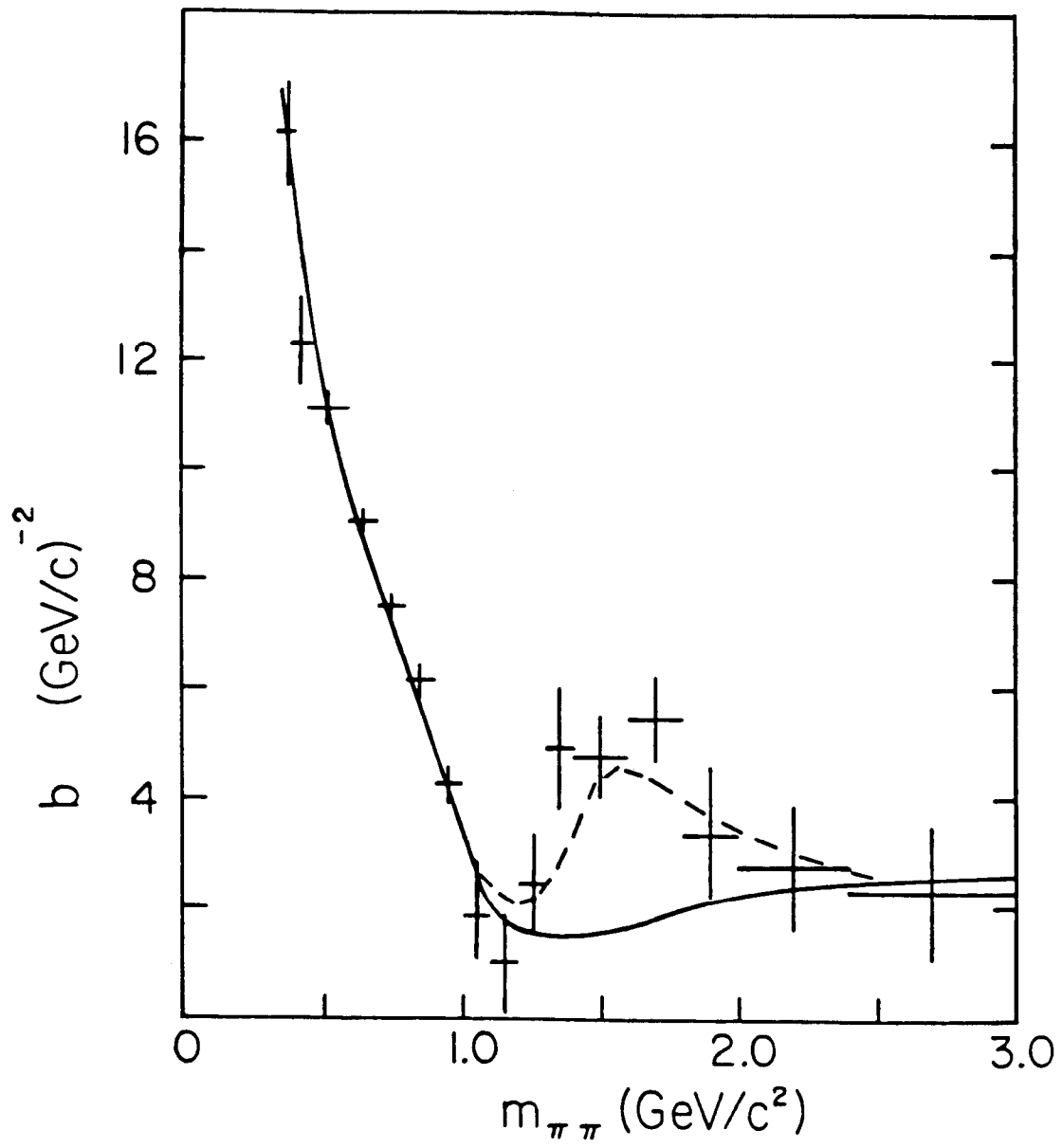


Fig. 2

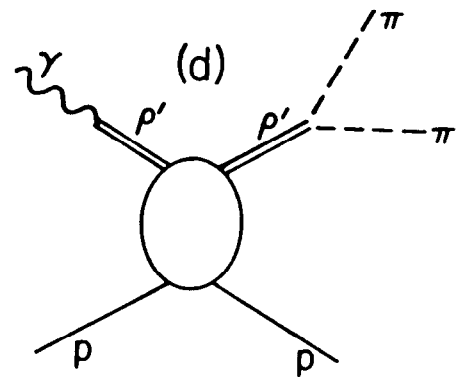
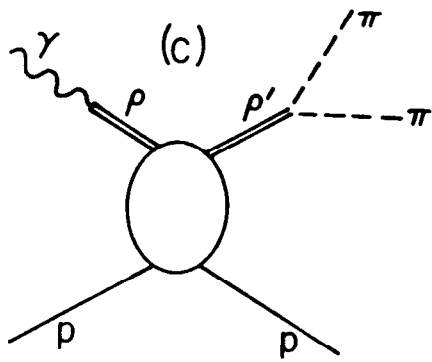
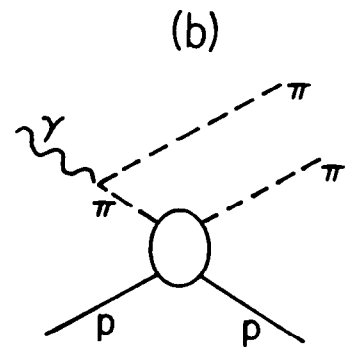
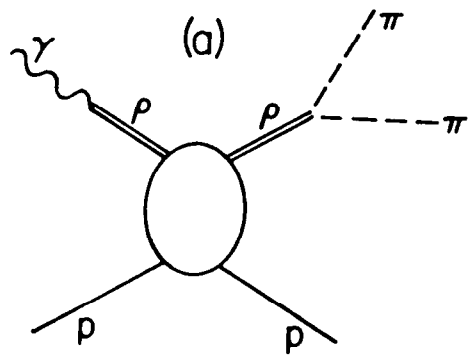


Fig. 3

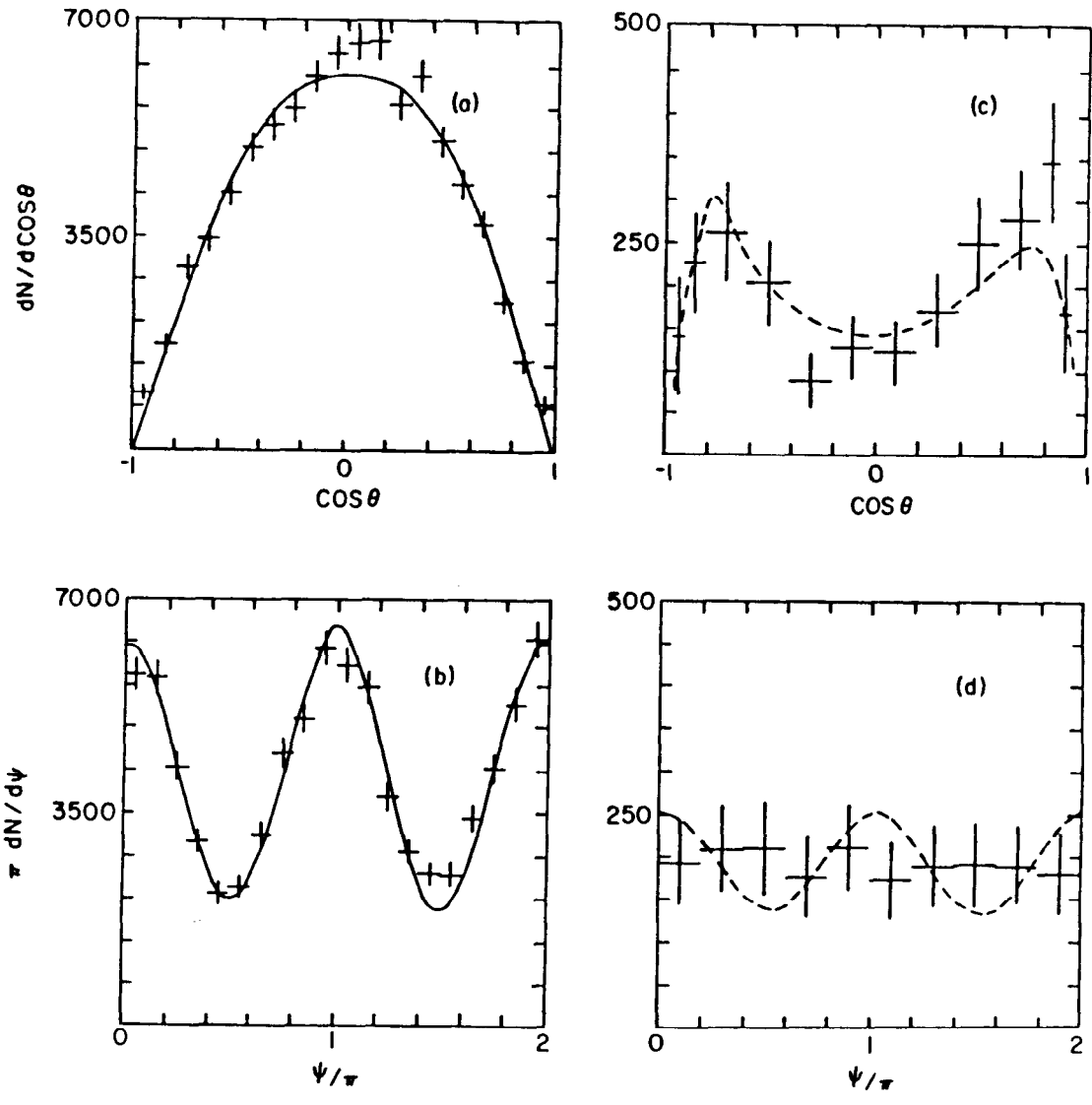


Fig. 4